Supplementary Materials:

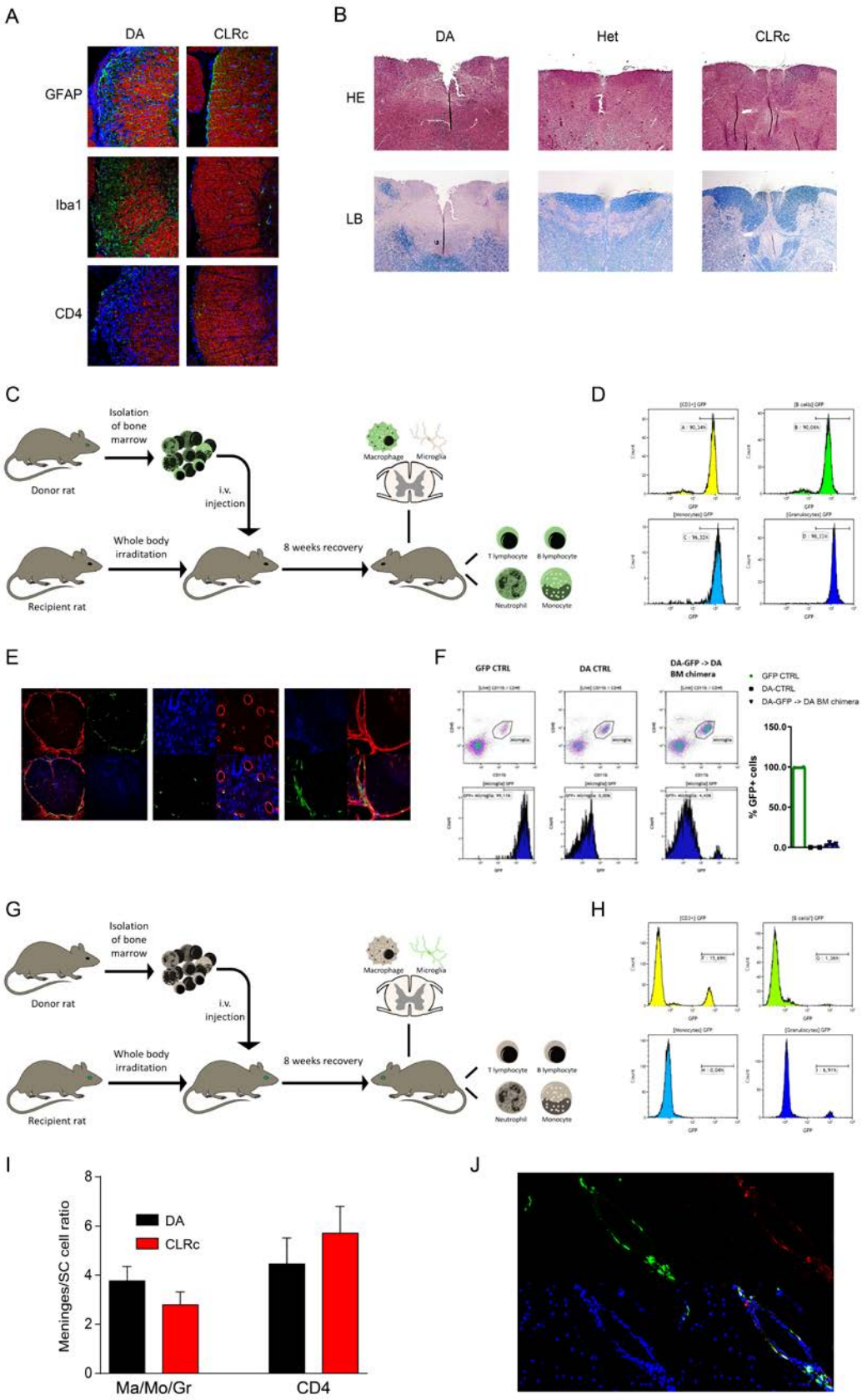

Fig. S1. The protective effect of CLRc is dependent on infiltrating immune cells but not microglia. (**A**) Immunofluorescent staining of DA and CLRc spinal cord day 24 p.i. Representative images of astrocytes (GFAP, green), microglia/macrophages (Iba1, green), and

T cells (CD4, green) along with myelin (fluoromyelin, red) and nuclei (DAPI, blue) (magnification 20X). (**B**) Histopathological analysis of brain (medulla) at day 29 p.i. Representative images of H&E and Luxol fast blue (LB) stainings (magnification 40X). (**C**) Schematic illustration of the bone marrow (BM) transfer (DA-GFP BM -> DA or CLRc) (**D**) Representative flow cytometry analysis of blood cells from BM transferred rats assessing level of reconstitution in DA-GFP -> DA rats at 8 weeks post transfer. (**E**) Immunofluorescent staining of sections from naïve BM-transferred rats assessing the replacement of meningeal and perivascular macrophages with donor BM-derived cells. BM-derived cells (GFP, green), meninges and blood vessels visualized by basal lamina staining (laminin, red), cell nuclei (DAPI, blue). Magnification for each panel, from left to right: 10X, 40X and 40X. (**F**) Flow cytometry analysis of spinal cord microglia from BM transferred rats assessing level of reconstitution in DA-GFP -> DA rats at 8 weeks post transfer. *Left*, representative flow cytometry plots. *Right*, quantification of GFP^+ microglia for DA-GFP (*n*=2), DA (*n*=2) and DA-GFP -> DA rats (*n*=4). (**G**) Schematic illustration of BM-transfer DA or CLRc BM -> DA-GFP. (**H**) Representative flow cytometry analysis assessing reconstitution efficiency in DA -> DA-GFP. (**I**) Ratio of the numbers of monocytes/macrophages/granulocytes and $CD4^+$ T cells infiltrating the meninges compared to spinal cord prior to EAE onset. Data are presented as mean ± SEM. (**J**) Immunofluorescent staining of immunized asymptomatic DA-GFP -> DA spinal cord day 31 p.i. assessing expression of Mcl (red) in GFP cells present in the meninges, nuclei stained with DAPI (blue) (magnification 40X).

A

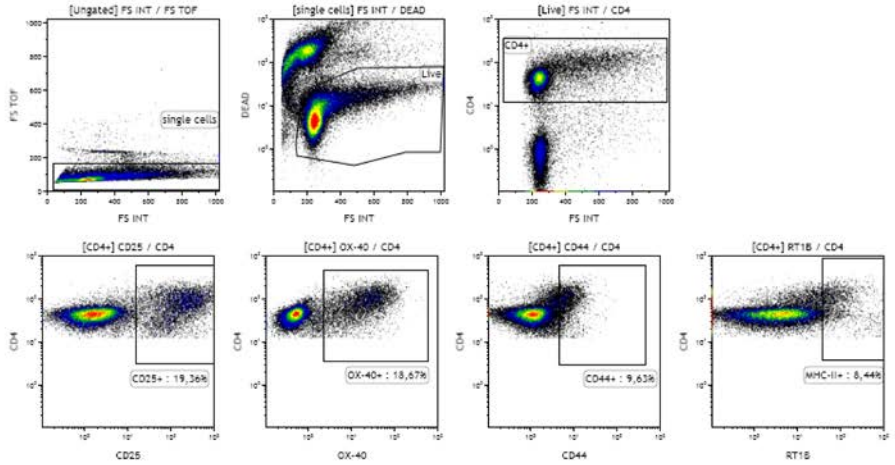
[Ungated] FS INT / FS TOF
single cells
FS TOF
FS INT
[single cells] FS INT / DEAD
Live
DEAD
FS INT
[Live] FS INT / CD4
CD4+
CD4
FS INT
[CD4+] CD25 / CD4
CD25+ : 19,36%
CD4
CD25
[CD4+] OX-40 / CD4
OX-40+ : 18,67%
CD4
OX-40
[CD4+] CD44 / CD4
CD44+ : 9,63%
CD4
CD44
[CD4+] RT1B / CD4
MHC-II+ : 8,44%
CD4
RT1B

B

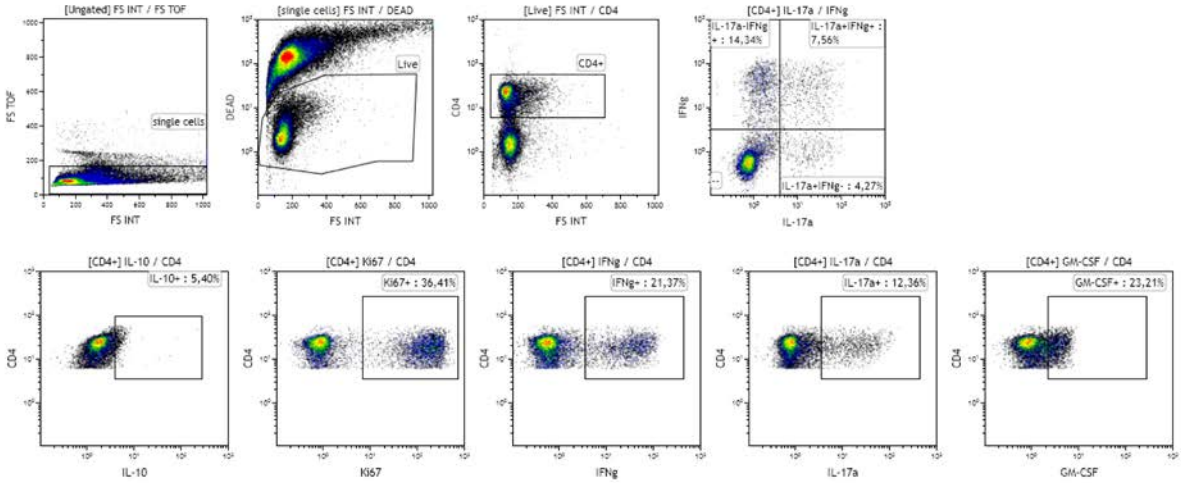
[Ungated] FS INT / FS TOF
single cells
FS TOF
FS INT
[single cells] FS INT / DEAD
Live
DEAD
FS INT
[Live] FS INT / CD4
CD4+
CD4
FS INT
[CD4+] IL-17a / IFNg
IL-17a-IFNg + : 14,34%
IL-17a+IFNg+ : 7,56%
IL-17a+IFNg- : 4,27%
IFNg
IL-17a
[CD4+] IL-10 / CD4
IL-10+ : 5,40%
CD4
IL-10
[CD4+] Ki67 / CD4
Ki67+ : 36,41%
CD4
Ki67
[CD4+] IFNg / CD4
IFNg+ : 21,37%
CD4
IFNg
[CD4+] IL-17a / CD4
IL-17a+ : 12,36%
CD4
IL-17a
[CD4+] GM-CSF / CD4
GM-CSF+ : 23,21%
CD4
GM-CSF

C

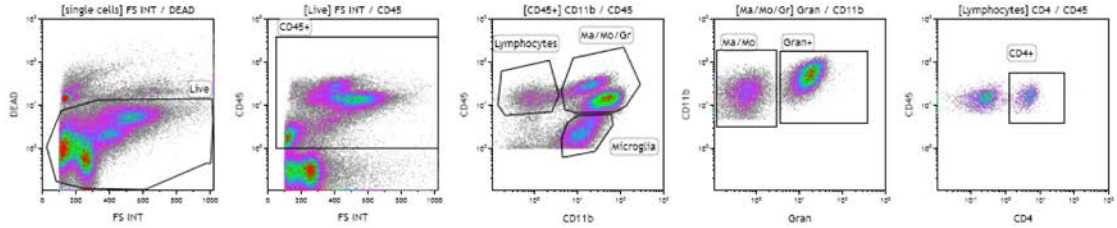
[single cells] FS INT / DEAD
Live
DEAD
FS INT
[Live] FS INT / CD45
CD45+
CD45
FS INT
[CD45+] CD11b / CD45
Lymphocytes
Ma/Mo/Gr
Microglia
CD45
CD11b
[Ma/Mo/Gr] Gran / CD11b
Ma/Mo
Gran+
CD11b
Gran
[Lymphocytes] CD4 / CD45
CD4+
CD45
CD4

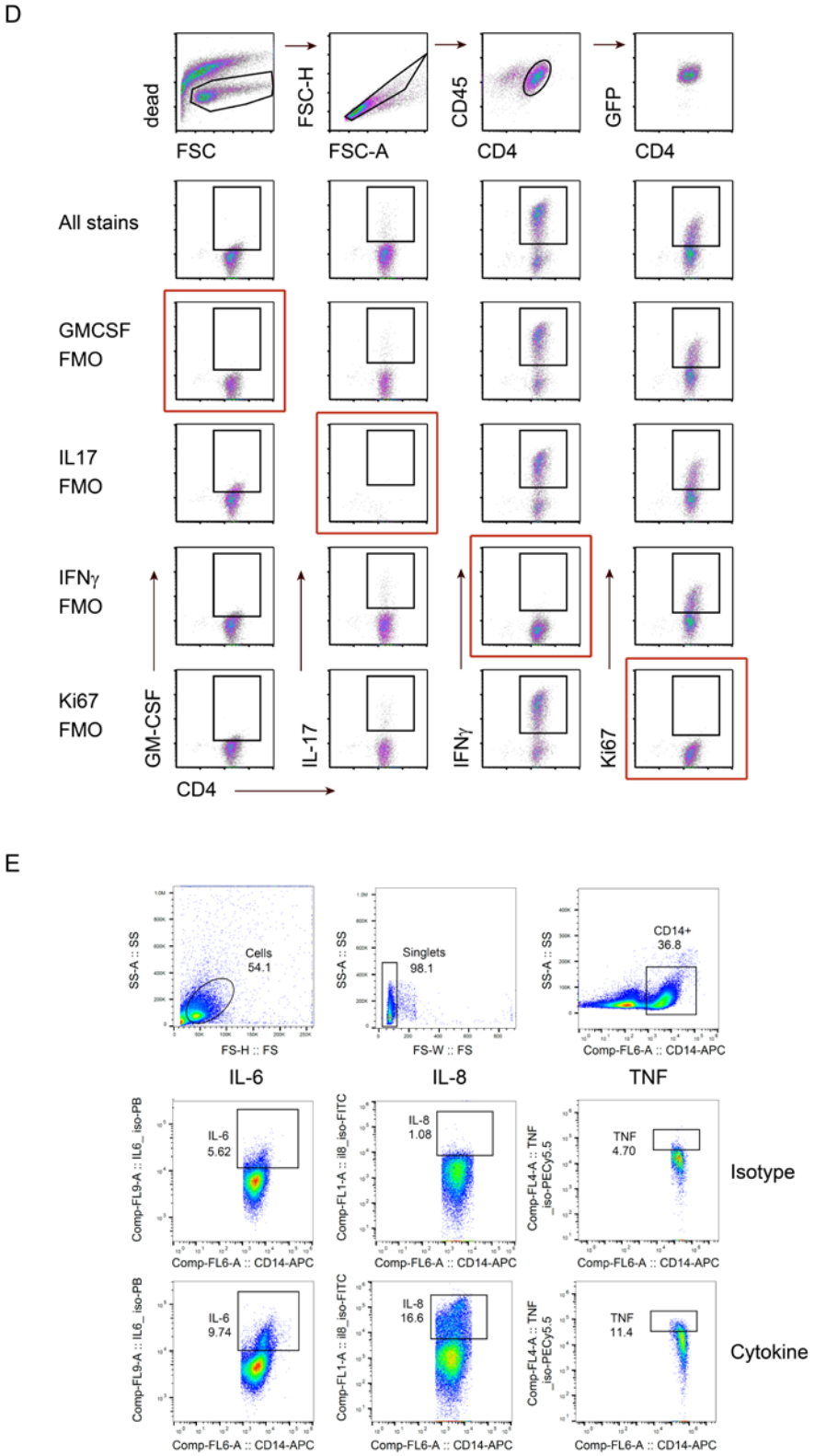

Fig. S2. Gating strategies for flow cytometry. (**A**) Gating strategy for CD4$^+$ T cell activation markers. (**B**) Gating strategy for intracellular cytokine expression and the proliferation marker Ki67. (**C**) Gating strategy for CNS immune cell subpopulations. (**D**) FMO stainings for assessment of rat CD4$^+$ T cell cytokine secretion. (**E**) Gating scheme for assessment of cytokine secretion from human monocytes.

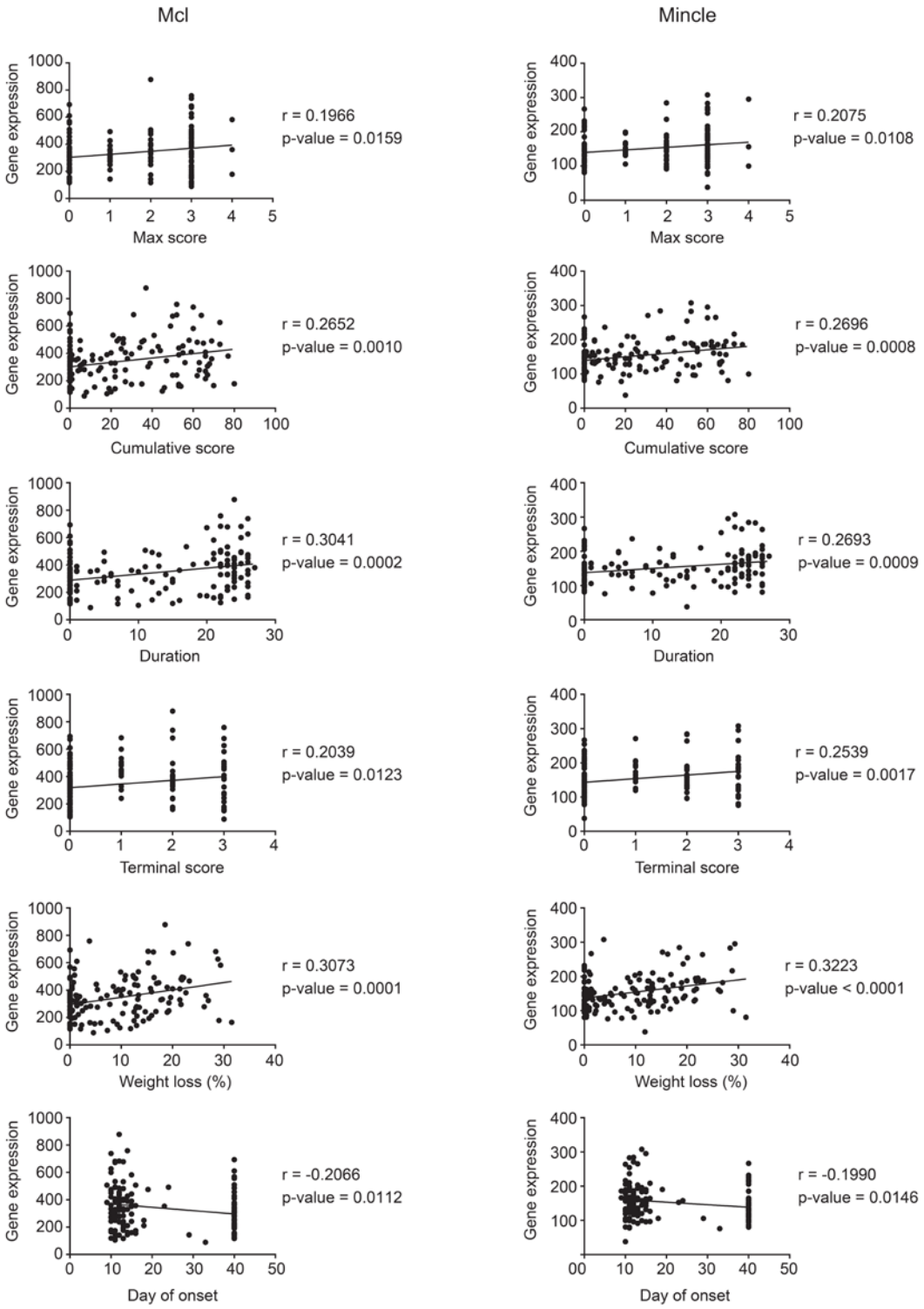

Fig. S3. Correlation between *Mcl/Mincle* expression and clinical EAE parameters. Gene expression from spleens of rats subjected to EAE (*n*=150) was correlated to clinical EAE phenotypes: maximal and cumulative score, disease duration, score at sampling (day 35 p.i.), maximal weight loss (in relation to day 7 p.i.) and day of disease onset. Significant correlations, using Pearson's correlation coefficient (and two-tailed p-value), are depicted in the figure together with lines from linear regression.

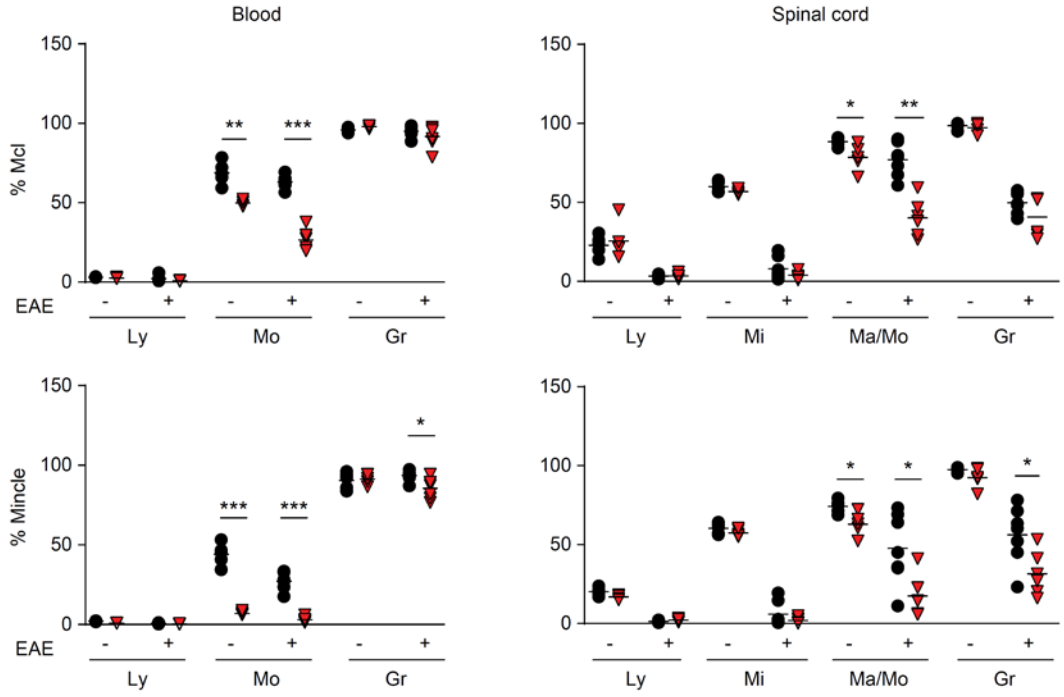

Fig. S4. Reduced frequency of Mcl- and Mincle-expressing cells in CLRc congenic rats. Flow cytometry analysis of cells isolated from peripheral blood and spinal cord of naive DA (n = 5) and CLRc (n = 5) rats and DA (n = 7) and CLRc (n = 6) rats 15 days p.i. The frequencies of Mcl- or Mincle-expressing lymphocytes, monocytes, granulocytes and spinal cord microglia were assessed. All comparisons were done with Mann–Whitney U test. *P < 0.05, **P < 0.01, ***P < 0.001.

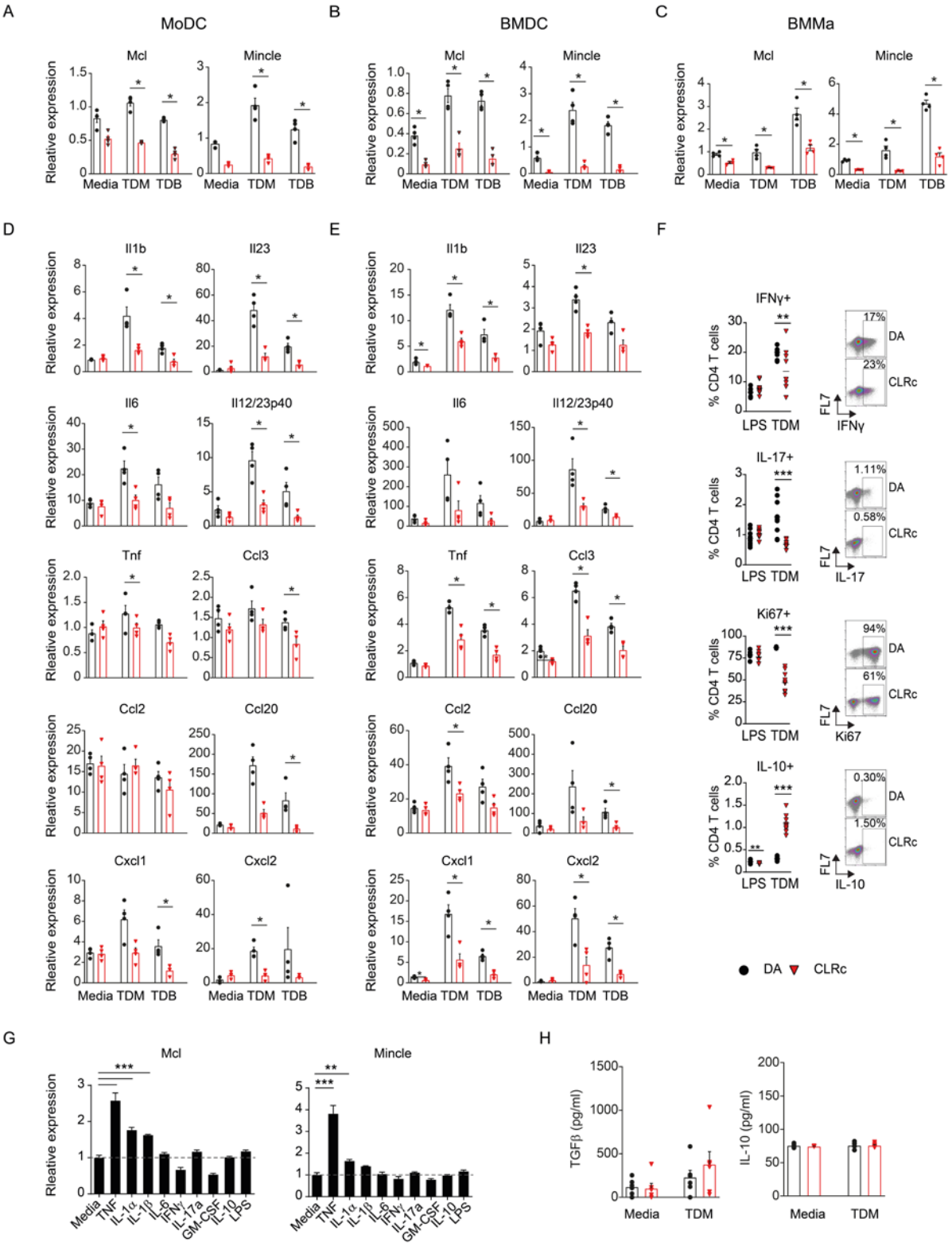

Fig. S5. CLRc bone marrow-derived macrophages and dendritic cells have a reduced response to Mcl/Mincle stimulation. Gene expression level (relative to *Actin*) of *Mcl* and *Mincle* in bone marrow-derived macrophages (BMMa) (**A**), MoDC (**B**) and bone marrow-derived dendritic cells (BMDC) (**C**) from DA (n = 4) and CLRc (n = 4) rats following 18h TDM, TDB and LPS stimulation in vitro (representative of two experiments). qPCR analysis

(relative to *Actin*) of MoDC (**D**) and BMDC (**E**) samples from DA (n = 4) and CLRc (n = 4) rats of transcripts induced in the Mcl and Mincle pathway (representative of two experiments). (**F**) Pooled resting $CD4^+$ cells isolated from lymph nodes of naïve rats were stimulated for 4 days with anti-CD3, anti-CD28 and supernatant from stimulated DA (n=8) or CLRc (n=8) BMDCs. Flow cytometry analysis of $CD4^+$ T cells assessing cytokine production and proliferation (representative of two experiments). (**G**) Mcl and Mincle expression assed by flow cytometry in BMMa from DA rats (n = 4) following cytokine stimulation. (**H**) ELISA for TGFβ and IL-10 from supernatants of DA (n = 6) and CLRc (n = 6) rats from TDM-stimulated MoDC. Data are presented as mean ± SEM. Comparisons were done with Mann–Whitney U test (**A**-**F** and **H**) and 1-way ANOVA with Dunnett's Multiple Comparison Test (**G**). *P < 0.05, **P < 0.01, ***P < 0.001.

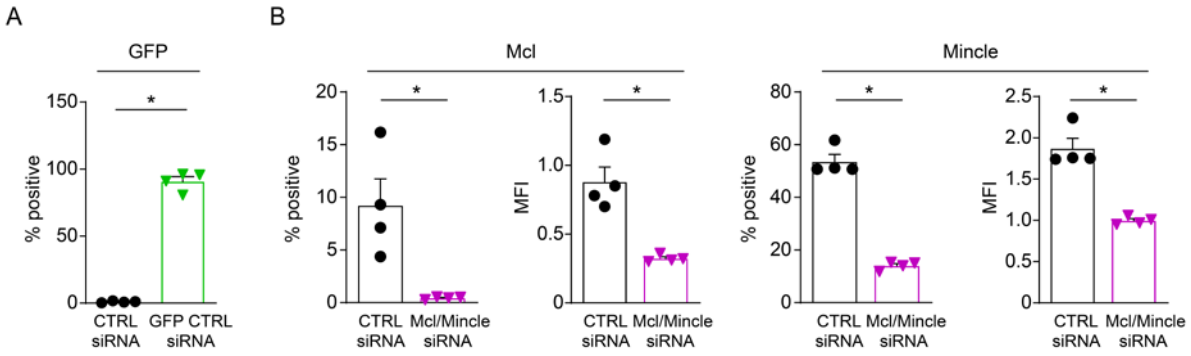

Fig. S6. Evaluation of siRNA silencing of *Mcl* and *Mincle* in vitro. Bone marrow-derived macrophages (BMMa) were treated with *Mcl/Mincle* or scrambled control siRNA. (**A**) Transfection efficiency of BMMa (n=4) transfection with control-siRNA or GFP-control siRNA assessed by flow cytometry. (**B**) Expression of Mcl and Mincle in BMMa assessed by flow cytometry, following treatment with *Mcl/Mincle* siRNA (n=4) or scrambled control siRNA (n=4). Data are presented as mean ± SEM. All comparisons were done with Mann–Whitney U test. *P < 0.05.

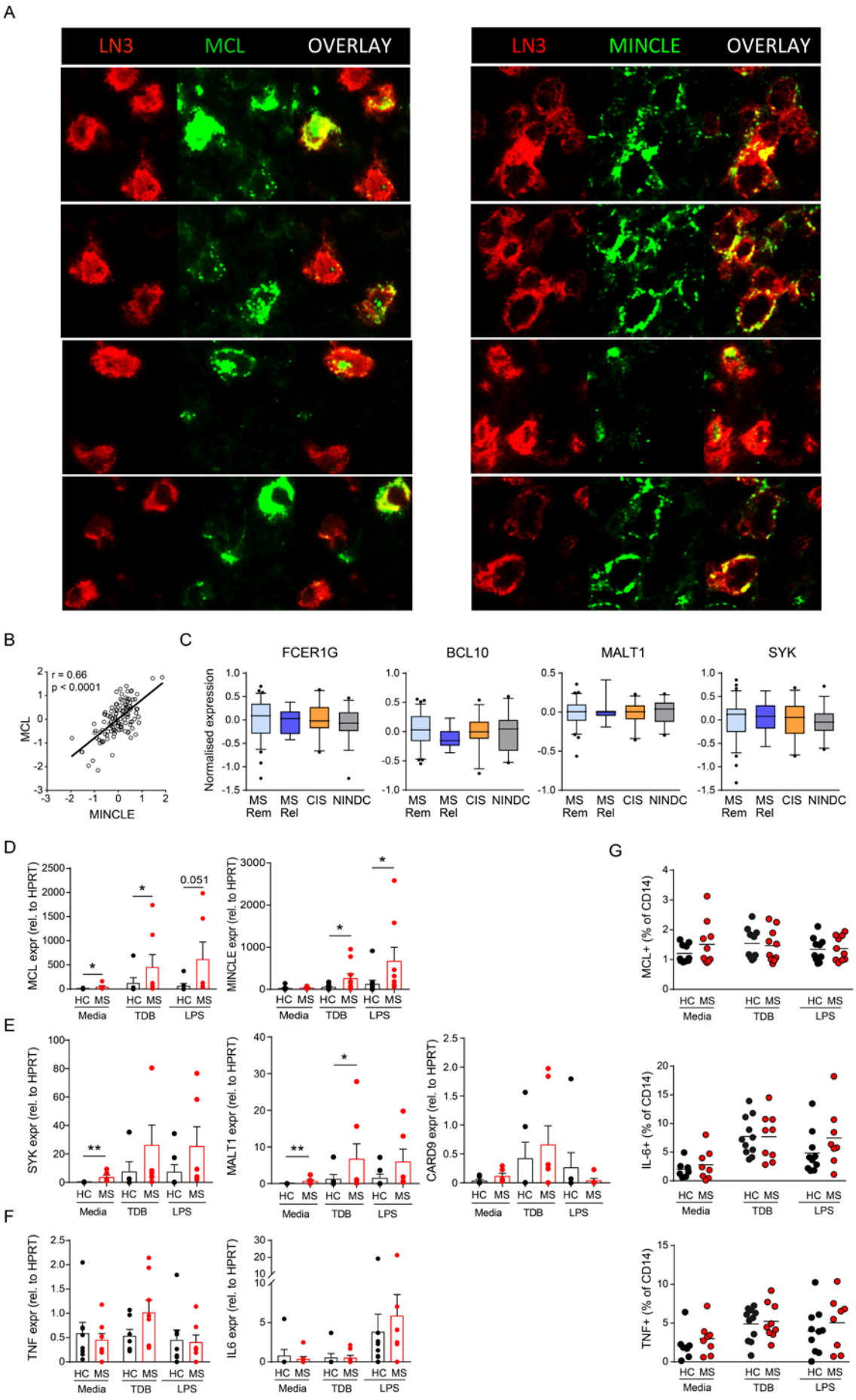
A
LN3
MCL
OVERLAY
LN3
MINCLE
OVERLAY
B
r = 0.66
p < 0.0001
MCL
MINCLE
C
FCER1G
BCL10
MALT1
SYK
Normalised expression
MS Rem
MS Rel
CIS
NINDC
D
MCL expr (rel. to HPRT)
MINCLE expr (rel. to HPRT)
0.051
HC MS
Media
TDB
LPS
E
SYK expr (rel. to HPRT)
MALT1 expr (rel. to HPRT)
CARD9 expr (rel. to HPRT)
F
TNF expr (rel. to HPRT)
IL6 expr (rel. to HPRT)
G
MCL+ (% of CD14)
IL-6+ (% of CD14)
TNF+ (% of CD14)

Fig. S7. Expression of the MCL/MINCLE signaling pathway in MS patients. (**A**) Additional representative immunofluorescent staining of MS lesions. MCL or MINCLE (green), HLA-DR expression (LN3, red), 40X magnification. (**B**) Expression analysis of PBMC from MS patients and non-inflammatory neurological disease controls (NINDCs) using RNA-sequencing. Expression analysis of PBMC from MS and CIS patients (*n*=115) shows co-expression of *MCL* and *MINCLE* in PBMC. (**C**) Expression of *FCER1G*, *BCL10*, *MALT1* and *SYK* comparing MS patients in remission (n=73), MS patients in relapse (*n*=14), CIS patients (*n*=28) and NINDCs (*n*=36). (**D, E** and **F**) qPCR analysis of *MCL*, *MINCLE*, *SYK*, *MALT1*, *CARD9*, *TNF* and *IL6* expression in $CD14^+$ enriched fraction from MS patients (*n*=8) and healthy controls (*n*=8) after 24 h stimulation. (**G**) Flow cytometry analysis of MCL, IL-6 and TNF production gated on $CD14^+$ monocytes from MS patients (*n*=9) and healthy controls (*n*=11) after 48 h stimulation. Data are presented as mean ± SEM or box-plots with whiskers representing 5-95 percentile. The following statistical tests were used: Pearson's correlation coefficient with two-tailed p-value (**B**), 1-way ANOVA with Dunnett's Multiple Comparison Test (**C**) and Mann-Whitney U test (**D**, **E**, **F** and **G**). **P* < 0.05; ***P* < 0.01.

Table S1. Genotyping of the CLRc region on rat chromosome 4.

SNP position (Mb)	159.707	159.746	159.823	159.884	159.906	159.961	160.578
Gene Symbol	*Dcir1*	*Dcar1*	*Dectin-2p*	*Mcl*	*Mincle*	*Vom2r48*	*Pex5*
	Clec4a	*Clec4b2*	*Clec4n*	*Clec4d*	*Clec4e*		
Genotype	DA	**PVG**	**PVG**	**PVG**	**PVG**	**PVG**	DA

Table S2. Correlation between CLR gene expression in spleen and different EAE phenotypes 35 days after EAE induction in (DAxPVG)xDA backcrossed rats (*n*=150).

	EAE (yes/no)	Max EAE score	Onset day	Cumulative EAE score	Duration	Score at day 35	Weight loss
Dcar1	0.05	0.06	0.02	0.05	0.07	0.04	0.05
Dectin-2p	-0.07	-0.03	0.04	-0.05	-0.06	-0.07	-0.09
Mcl	0.20*	0.19*	-0.22**	0.25**	0.28***	0.22**	0.29***
Mincle	0.23**	0.20*	-0.21**	0.26**	0.28***	0.25**	0.31***
Vom2r48	-0.02	0.02	0.06	-0.00	-0.00	0.04	-0.05

Numbers indicate Pearson's correlation coefficient and statistical significance with * $p<0.05$, ** $p<0.01$, *** $p<0.001$.

Table S3. Baseline characteristics of the human brain cohort.

Patient ID	Lesion type	Age (years)	MS type	Gender	Post-mortem delay (h)	Target
MS 1	Chronic active	56	n.a.	n.a.	10:10 h	MCL/MINCLE
MS 2	Chronic active	66	SPMS	F	6 h	MINCLE
MS 3	Active	77	PPMS	M	4:15 h	MCL/MINCLE
MS 4	Active	61	n.a.	n.a.	10:55 h	MCL
MS 5	Active	51	SPMS	M	11:00 h	MCL

n.a. data not available

Table S4. Baseline characteristics of the human RNA-sequencing cohort.

	RRMS relapse (n=14)	RRMS remission (n=73)	PPMS (n=7)	SPMS (n=8)	CIS (n=28)	NINDC (n=36)
Age mean, (SD)	35 (12.4)	40 (12.4)	51 (7.5)	52 (8.4)	36.5 (10.4)	40.9 (12.5)
Female sex, n (%)	9 (64.3)	52 (71.2)	1 (14.3)	5 (62.5)	25 (89.3)	29 (80.5)
EDSS, mean (SD)	2.7 (1.2)	2.0 (1.3)	4.2 (1.1)	4 (0.7)	1.4 (1.0)	n.a.
Years since diagnosis, mean (SD)	1.7 (4.6)	1.7 (4.3)	3 (4.8)	4.9 (9.7)	0.4 (0.7)	n.a.
Immunomodulatory treatment, n (%)	0 (0)	0 (0)	0 (0)	0 (0)	0 (0)	n.a.

n.a. not applicable

Table S5. Baseline characteristics of the human in vitro stimulation cohort.

	MS (n=9)	HC (n=11)	p-value
Age (mean, SD)	57.6 (5.2)	49.9 (13,0)	0.03
Female sex (n, %)	3 (33 %)	4 (36 %)	n.s.
Tysabri treatment (n, %)	9 (100%)	n.a.	n.a.
RRMS, remission (n, %)	9 (100%)	n.a.	n.a.
EDSS (mean, SD)	2.1 (1.4)	n.a.	

n.a. not applicable, n.s. not significant